An Accurate Semi-Analytic Finite Difference Scheme for Two-Dimensional Elliptic Problems with Singularities

Z. Yosibash, M. Arad, A. Yakhot, G. Ben–Dor
Pearlstone Center for Aeronautical Engineering Studies
Dept. of Mechanical Engineering
Ben–Gurion University of the Negev
Beer–Sheva, Israel

A high-order semi-analytic finite difference scheme is presented to overcome degradation of numerical performance when applied to two-dimensional elliptic problems containing singular points. The scheme, called Least-Square Singular Finite Difference Scheme (L-S SFDS), applies an explicit functional representation of the exact solution in the vicinity of the singularities, and a conventional finite difference scheme on the remaining domain. It is shown that the L-S SFDS is "pollution" free, i.e., no degradation in the convergence rate occurs because of the singularities, and the coefficients of the asymptotic solution in the vicinity of the singularities are computed as a by-product with a very high accuracy. Numerical examples for the Laplace and Poisson equations over domains containing re-entrant corners or abrupt changes in the boundary conditions are presented. © 1998 John Wiley & Sons, Inc. Numer Methods Partial Differential Eq 14: 281–296, 1998

I. INTRODUCTION

Standard high-order finite difference schemes (FDS) are very efficient in solving elliptic partial differential equations (PDEs) [1–5], except for problems containing singularities, where their high-order convergence rate deteriorates [4, 5]. Singular points may arise on the boundary from an abrupt change of boundary conditions or a re-entrant corner, and first derivatives of the exact solution tend to infinity as the distance from these points tends to zero. In the presence of such singularities, standard high-order FDSs become inaccurate, and reasonable engineering accuracy is often impossible, or at least is very costly to obtain due to the need of a highly refined mesh. FDSs have been modified in various ways in order to overcome this difficulty, see, e.g., [6]. The schemes suggested, however, suffer from either inefficiency due to the requirement of a large number of grid points in the neighborhood of singularities, or they must be modified in ways

that are very difficult or even impossible to incorporate into standard finite difference computer programs.

This article presents a semi-analytic method for obtaining accurate solutions to elliptic problems with singularities. The method is based on the use of known expansions of the solution in the vicinity of singular points. We show several examples where the difficulties may be overcome by a simple yet efficient scheme, provided that the form of the asymptotic series for the solution in the neighborhood of the singular point is known *explicitly*. The developed scheme overcomes the deterioration of the high-order FDS convergence rate (due to singularities), and at the same time provides the coefficients of the asymptotic series (which determine the analytic solution in the vicinity of the singular point) with high accuracy. These coefficients are of major engineering importance. We demonstrate the method on the basis of two-dimensional Laplace and Poisson equations with analytic forcing functions on polygonal domains containing re-entrant corners or abrupt changes of boundary conditions. These problems have been chosen because they are simple enough for demonstration purposes, yet contain all the essential properties that are common to elliptic boundary value problems. From an engineering point of view, the Laplace and Poisson equations describe several interesting problems such as steady state heat transfer in an unsmooth domain, Poiseuille flow along a straight duct of cross-section containing re-entrant corners, the Saint Venant torsion of a bar having an unsmooth cross-section, the deflection of a membrane with a free half-edge, etc.

Similar methods to the one presented here, in the framework of boundary and finite element methods, have been analyzed mathematically in detail in the past, and the reader is referred to [7, 8] and the references therein. In [7, 8] the results are highly influenced by the number of terms in the singular asymptotic series N, and the condition number increases considerably as N increases. This is not the case in the present study, as will be shown in Section III.A.

The notation, preliminaries, and techniques are formulated in Section II. In Section III we present the results of three numerical examples: the well-known Motz problem [9], and the Laplace and Poisson equation over an L-shaped domain [10]. We conclude with summary and conclusions in Section IV.

II. FORMULATION

A. Notations and Preliminaries

We consider the Poisson equation

$$\nabla^2 u(x, y) = -f(x, y) \quad in \quad \Omega \tag{1}$$

$$B_i(u) = 0 \quad on \quad \Gamma_i \quad i = 1, 2 \tag{2}$$

$$B_i(u) = d_i(x, y) \quad on \quad \Gamma_i \quad i \neq 1, 2, \tag{3}$$

where $d_i(x, y)$ are smooth functions on the boundaries, and B_i is the trace operator for *Dirichlet boundary conditions*, and $\partial/\partial n$ for *Neumann boundary conditions*, $\mathbf{n}$ denotes the outward normal vector to the boundary. The solution to the above problem in the vicinity of a singular point takes the form

$$u = u_H + u_P.$$

For polynomial functions f, or simple ones, it is possible to find explicitly a particular solution, u_P, which satisfies (1) identically.

The analytic form of the homogeneous solution, u_H (satisfying the Laplace equation $\nabla^2 u_H = 0$), in a two-dimensional domain Ω in the vicinity of a singular point is best understood and is given in the form of an asymptotic series with unknown coefficients [11, 12]:

$$u_H = \sum_{i=1}^{N} \sum_{s=0}^{S} \sum_{m=0}^{M} A_{ism} f_{ism}(\theta) r^{\alpha_i + m} \ln^s(r) + u_{smooth}, \tag{4}$$

r and θ being the polar coordinates of a system located in the singular point. α_i are the eigenvalues (real numbers in the case of the Laplace problem) and $f_{ism}(\theta)$ are the eigen-functions, which are analytic. The function u_{smooth} belongs to the Sobolev space $H^q(\Omega)$, where q depends on N, and can be made as high as required providing that N is large enough. Except for special cases (when α_i is an integer, or when the multiplicity of an eigenvalue is higher than the multiplicity of the corresponding eigen-function), $S = 0$. M is either 0, or a positive integer when the boundary near the singular point (at the vertex) is curved. Herein only straight boundaries in the vicinity of the singular point will be addressed, and the special cases where $\ln r$ terms appear will not be treated; therefore, we consider (4) in the simplified form

$$u_H = \sum_{i=1}^{N} A_i r^{\alpha_i} f_i(\theta) + u_{smooth}. \tag{5}$$

The eigen-pairs are uniquely determined by the geometry, the boundary conditions along boundaries intersecting in the singular point, and material data. Note that if $\alpha_i < 1$, the corresponding ith term in the expansion (4) for ∇u is unbounded as $r \to 0$. In some cases, the eigen-functions $f_i(\theta)$ cannot always be computed explicitly, and numerical approximations to f_i and α_i (cf. [13–16]) have to be used. We can think of the coefficients A_i of these terms as analogous to the stress intensity factors of elasticity. We generalize this terminology, and refer to all coefficients A_i, whether or not the corresponding terms in (4) are singular, as generalized flux intensity factors (GFIFs). The analogous coefficients in elasticity are called generalized stress intensity factors (GSIFs). The GSIFs are very important from an engineering point of view, because they are related to failure theories.

Let $\partial\Omega = \cup_i \Gamma_i$, where Γ_i are straight lines called edges. These edges intersect at points called vertices. The two boundaries intersecting in the singular point of interest are denoted by Γ_1 and Γ_2, see Fig. 1.

When f in (1) is not a polynomial or a simple function for which u_P could be found explicitly, the following approach can be adopted. Under mild regularity restriction on f in the vicinity of singularities, one may expand f in a series of the form

$$f = \sum_{i=0}^{\infty} r^i \phi_i(\theta). \tag{6}$$

By the shift theorem, the particular solution u_P for the cases that $i + 2 \neq \alpha_j \forall i, j$ is

$$u_P = \sum_{i=0}^{\infty} r^{i+2} \psi_i(\theta), \tag{7}$$

where $\psi_i(\theta)$ are constructed from $\phi_i(\theta)$, by solving an ordinary differential equation in θ. Otherwise, for each α_j that satisfies $i + 2 = \alpha_j$, the series expansion (7) will contain a term of the form

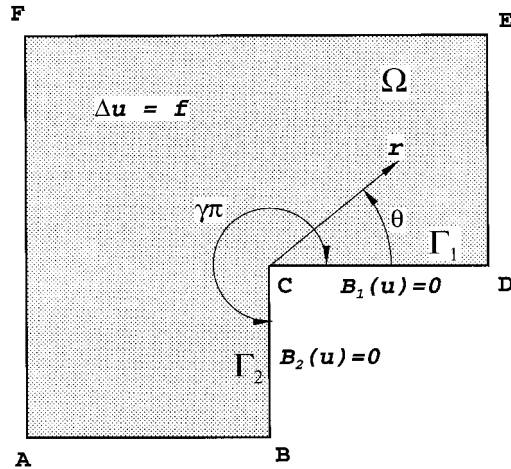$$r^{i+2}[c_j \ln(r) f_j(\theta) + \psi_i(\theta)], \tag{8}$$

FIG. 1.   Domain with a re-entrant corner and notations.

with c_j chosen such that the ''Fredholm's Alternative'' is satisfied (see [17, pp. 78–80]). It is important to note that $\psi_i(\theta)$ can be constructed as a linear combination of $f_i(\theta)$ as shown in [18, Chapt. 8].

We consider polygonal domains with boundaries parallel to the Cartesian axes, so that we can apply a finite difference grid that is free of curved boundary representation errors, and does not require a special scheme near aligned boundaries. This enables us to concentrate on the influence of the singularities alone on the performance of the FDS. The grid is uniform both in x and y directions, and the distance between two adjacent grids parallel to one of the axes is denoted by h.

B. Finite Difference Scheme

Considering the Poisson Eq. (1), the high-order finite difference scheme used in our computation is the explicit nine-point stencil with $h_x = h_y = h$, which gives a truncation error of $\mathcal{O}(h^8)$ over a square mesh (i.e., a convergence rate of $\mathcal{O}(h^6)$). For any grid point denoted by the indices i, j, the discretization scheme is given by [2, 5, 19]

$$
\frac{1}{6h^2}[4(u_{i-1,j} + u_{i,j-1} + u_{i+1,j} + u_{i,j+1})
$$
$$
+ (u_{i-1,j-1} + u_{i+1,j-1} + u_{i+1,j+1} + u_{i-1,j+1}) - 20u_{i,j}]
$$
$$
= \left[1 + \frac{2h^2}{4!}\nabla^2 + \frac{2h^4}{6!}\left(\nabla^4 + 2\frac{\partial^4}{\partial x^2 \partial y^2}\right)\right]f_{i,j}. \tag{9}
$$

The fourth-order discretization scheme based on the nine-point stencil with $h_x \neq h_y$ is presented in [20].

Neumann boundary condition implementation requires a special technique for retaining the $\mathcal{O}(h^6)$ order of the overall scheme. Assume that the Neumann boundary condition $\frac{\partial}{\partial y}u(x, y = 0) = g(x, y = 0)$ is imposed on the boundary $y = 0$. For any grid point on this boundary, (9)

becomes

$$\frac{1}{6h^2}[4(u_{i-1,0} + u_{i,-1} + u_{i+1,0} + u_{i,1}) + (u_{i-1,-1} + u_{i+1,-1} + u_{i+1,1} + u_{i-1,1}) - 20u_{i,0}]$$
$$= \left[1 + \frac{2h^2}{4!}\nabla^2 + \frac{2h^4}{6!}\left(\nabla^4 + 2\frac{\partial^4}{\partial x^2 \partial y^2}\right)\right]f_{i,0}. \quad (10)$$

Grid points with the index $j = -1$ denote fictitious (dummy) nodes, which lie outside the computational domain. The Taylor series expansion for a node at $j = \pm 1$ is given by

$$u_{i,\pm 1} = u_{i,0} + \sum_{m=1}^{\infty} \frac{(\pm 1)^m}{m!} h^m \frac{\partial^m u_{i,0}}{\partial y^m}. \quad (11)$$

Using (11) one obtains

$$u_{i,1} - u_{i,-1} = 2\sum_{m=1}^{\infty} \frac{h^{2m-1}}{m!} \frac{\partial^{2m-1} u_{i,0}}{\partial y^{2m-1}}. \quad (12)$$

By repeated differentiation m times with respect to y of (1), and rearranging it, the following recurrent form is obtained:

$$\frac{\partial^{2m-1} u}{\partial y^{2m-1}} = \frac{\partial^{2m-3}}{\partial y^{2m-3}}\left[f - \frac{\partial^2 u}{\partial x^2}\right], \quad m = 2, 3, \cdots \quad (13)$$

Assume for simplicity that $f(x,y)$ in (13) is constant (the techniques outlined here can be generalized to any analytic function f), then, applying recursively (13) for the grids on the boundary $y = 0$ yields

$$\frac{\partial^{2m-1} u_{i,0}}{\partial y^{2m-1}} = -\frac{\partial^2}{\partial x^2}\frac{\partial^{2m-3} u_{i,0}}{\partial y^{2m-3}} = \cdots = (-1)^{m-1}\frac{\partial^{2m-2} g(x_i)}{\partial x^{2m-2}}, \quad m = 1, 2, \cdots \quad (14)$$

Substituting (14) into (12) gives an explicit expression for the dummy nodes

$$u_{i,-1} = u_{i,1} - 2\sum_{m=1}^{\infty} \frac{h^{2m-1}}{m!}(-1)^{m-1}\frac{\partial^{2m-2} g(x_i)}{\partial x^{2m-2}}. \quad (15)$$

For $\mathcal{O}(h^8)$ truncation term, four terms in the series (15) are sufficient:

$$u_{i,-1} = u_{i,1} - 2\sum_{m=1}^{4} \frac{h^{2m-1}}{m!}(-1)^{m-1}\frac{\partial^{2m-2} g(x_i)}{\partial x^{2m-2}}. \quad (16)$$

Substitution of (16) for the dummy nodes in (11) provides a sixth-order accuracy discretization when Neumann boundary conditions are applied. In the particular case where $g(x) = 0$ and $f(x,y)$ is constant, (16) reduces to $u_{i,-1} = u_{i,1}$, and the nine-point stencil becomes

$$\frac{1}{6h^2}[4(u_{i-1,0} + u_{i+1,0} + 2u_{i,1}) + (2u_{i+1,1} + 2u_{i-1,1}) - 20u_{i,0}] = const. \quad (17)$$

It should be noted that the same procedure may be applied twice (in the neighborhood of an intersection of two boundaries) to obtain a discretization at Neumann corners.

   The FDS loses its $\mathcal{O}(h^6)$ convergence rate in the presence of singularities, as will be demonstrated by a numerical example. To overcome this difficulty, a new technique called Singular Finite Difference Scheme (SFDS), which employs the analytic form of the exact solution in the vicinity of the singularity, is developed.

C. Singular Finite Difference Scheme

Consider for example the L-shaped domain in Fig. 1, having a singular point at vertex C. An artificial sub-domain denoted by Ω_S is considered, and the common boundary with Ω is denoted by Γ_S, see Fig. 2. The boundary Γ_S is constructed along the grid points, such that Ω_S is defined as $\{(x,y)|(x,y) \in \Omega, |x| < Ex, |y| < Ey\}$. In Ω_S no grid-mesh is employed, instead, u at any given point is represented by the analytic solution given in (5), i.e., by a series of N terms with A_i, $i = 1, \ldots, N$ being unknowns. Only in $\Omega - \Omega_S$ the discretization scheme (9) is employed. Let us say, for example, that there are NG grid points in $\Omega - \Omega_S$ (e.g., 99 grid points in Fig. 2). The scheme for each grid laying on Γ_S has to include at least a point in Ω_S, so that the series coefficients A_i become a part of the unknowns in the algebraic system of equations. Thus, one obtains an under-determined system of NG equations with $NG + N$ unknowns.

There are two possible ways for generating the N additional equations necessary to solve the undetermined system: (a) Collocation of arbitrary points on Γ_S, or (b) Least-Squares for all points on Γ_S. Although the collocation technique does not provide results of acceptable accuracy, we describe it and demonstrate the results on an example problem in Section III.

Collocation: The solution $u_{i,j}$ at each grid on Γ_S, satisfying the FDS (9), satisfies also (5), i.e., has the analytic form of the solution in the vicinity of the singular point. If N terms are considered in the analytic expression, one has to have at least: (a) $N + 2$ grid points along Γ_S if Dirichlet B.C.s are applied on both boundaries Γ_1 and Γ_2, (b) $N + 1$ grid points along Γ_S if Neumann B.C.s are applied on Γ_1 or Γ_2, (c) N grid points along Γ_S if Neumann B.C.s are applied on both Γ_1 and Γ_2. (The grid points on Γ_1 and Γ_2 cannot be used for collocation if Dirichlet boundary conditions are prescribed.) Thus, additional N algebraic equations of the form

$$u_{i,j} - (u_P)_{i,j} = \sum_{k=1}^{N} A_k r_{i,j}^{\alpha_k} f_k(\theta_{i,j}) \tag{18}$$

have to be added to the system of NG equations. In (18) $r_{i,j}$ (resp. $\theta_{i,j}$) represents the radius vector (resp. the angle shown in Fig. 1) from the vertex to the grid point i,j. The choice of the grid points along Γ_S for which (18) is applied is made arbitrarily, and the results are virtually insensitive to the location of the grid points.
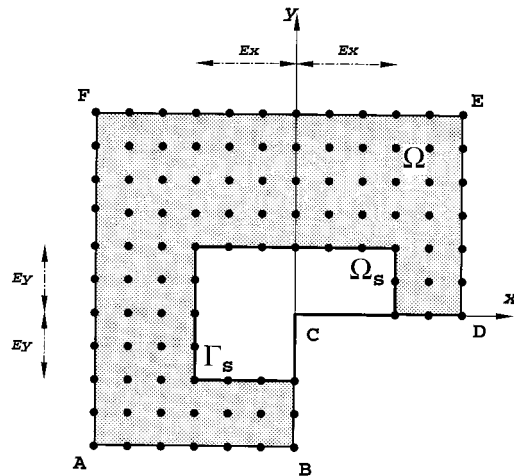

FIG. 2.   Notations for the SFDS.

Least Squares: Here all the grids along Γ_S are considered, and at each grid it is required that Eq. (18) be satisfied. It is essential that the number of the grid points along Γ_S be greater than $N + i$, where i is either 0, 1, or 2, as explained previously. Thus, an over-determined set of equations is obtained, such that a procedure of least squares is applied. We define:

$$\mathcal{B} = \sum_i \sum_j \left[u_{i,j} - (u_P)_{i,j} - \left(\sum_{k=1}^N A_k r_{i,j}^{\alpha_k} f_k(\theta_{i,j}) \right) \right]^2, (x_i, y_j) \in \Gamma_S. \tag{19}$$

$\mathcal{B}$ obtains a minimum when the coefficients A_k are the best approximation to the exact values. Thus, we have to consider:

$$\frac{\partial \mathcal{B}}{\partial A_k} = 0 \quad k = 1, 2, \cdots N. \tag{20}$$

(20) provides a system of N equations, which is added to the NG system of equations, thus providing a complete system for the $N + NG$ unknowns.

Empirical connection between N and h: For obtaining a connection between the number of terms in the series used in Ω_S and h in $\Omega - \Omega_S$, it is natural to argue that the FDS truncation error should be of the same magnitude as the series truncation error. This is equivalent to requiring that second derivatives have the same orders of magnitude:

$$\mathcal{O}(h^6) = \mathcal{O}(R^{\alpha_N - 2}), \tag{21}$$

where R is the distance to the points in Ω_S that are used for the FDS, i.e., $R = \mathcal{O}(Ex - h)(Ex \approx Ey)$. From (21) the following connection is obtained:

$$\alpha_N = \mathcal{O}\left[2 + \frac{6 \log(h)}{\log(Ex - h)} \right]. \tag{22}$$

Hence, one should use N terms in the series so that the next term, which is omitted, is approximately given by (22) as a function of h and Ex. It should be noted that N cannot be greater than the number of grids along Γ_S. If (22) requires a larger number of terms in the series expansion, this number should be limited to the number of grids along Γ_S.

Remark 1. An FDS results in a system of algebraic equations that may be represented in a matrix form $[K]\mathbf{u} = \mathbf{b}$, where $[K]$ is a sparse symmetric matrix with a low bandwidth. This enables efficient solvers for the solution of the matrix equations. The addition of the series coefficients to the matrix $[K]$ increases the band-width of the generated matrix. However, if the grids on Γ_S and the grids in their vicinity are numbered properly, this does not cause a significant deterioration in the efficiency. Herein, due to the small dimension of the matrix $[K]$, no special numbering strategy has been considered.

III. NUMERICAL EXAMPLES

Abilities of the L-S SFDS are illustrated on three example problems for which previous results are available. Two of them concern the Laplace equation, the singularity being caused by an abrupt change in the specified boundary conditions in the first case, and by a re-entrant corner on the boundary in the second. The third is the Poisson equation over an L-shaped domain, which is of engineering importance. These problems were chosen because, in each case, the domain has a simple form that has enabled results of high accuracy to be obtained using a variety of methods,

which are of less general applicability than the current scheme. We will, therefore, take these results as benchmarks against which the accuracy of the current results may be assessed.

A. ''Motz Problem''—Laplace Equation

We consider the solution of the Laplace equation over the region $-1 < x < 1, 0 < y < 1$ shown in Fig. 3 subject to the boundary conditions:

$$u = 0 \text{ on } -1 \le x \le 0, y = 0$$

$$u = 500 \text{ on } x = 1, 0 \le y \le 1$$

$$\partial u/\partial n = 0 \text{ elsewhere on the boundary.} \tag{23}$$

The discontinuity at the origin in the boundary conditions along the line $y = 0$ results in a singularity at this point. The asymptotic expansion of the solution about the origin is of the form [9]

$$u = \sum_{i=1}^{\infty} A_i r^{i-1/2} \cos[(i - 1/2)\theta]. \tag{24}$$

This problem was first formulated by Motz [9] in a slightly different form.

Loss of high-order convergence of the FDS: First, we demonstrate that when the singular point is not properly treated, the $\mathcal{O}(h^6)$ convergence rate is lost not only in the neighborhood of the singularity, but also where the solution is smooth. This phenomenon, known as ''pollution,'' has been demonstrated long ago in [21]. Due to ''pollution,'' the convergence in L_∞ norm, as $h \to 0$, is at most $\mathcal{O}(h^{2\alpha_{\min}-\epsilon}), \epsilon > 0$ can be arbitrary small, which for the Motz problem becomes

$$\|u_h - u_{EX}\|_{L_\infty,\Omega-\Omega_S} \overset{\text{def}}{=} \|e\|_{L_\infty,\Omega-\Omega_S} \le Ch^{1-\epsilon}. \tag{25}$$

Over the whole domain we use a grid-mesh containing NGx grid points in the x-direction and NGy grid points in the y-direction. Four different meshes are studied with $(NGx, NGy) = (11, 6), (21, 11), (41, 21), (81, 41)$. We define the Ω_S sub-domain by $Ex = Ey = 0.4$. The so-called ''exact'' solution over $\Omega - \Omega_S$ is obtained numerically by solving the problem on $\Omega - \Omega_S$ with a (161, 81) mesh, applying on the boundary Γ_S the exact series truncated after 20 terms. We define the RMS_h norm (equiv. L_h^∞) as the norms corresponding to the Root-mean-square norm discretized and evaluated at the data generated at the grid points. The pollution effect is clearly seen in Fig. 4, where we plot the RMS_h measure of the error and the error in L_h^∞ norm
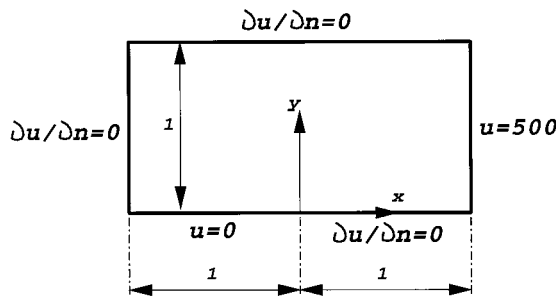

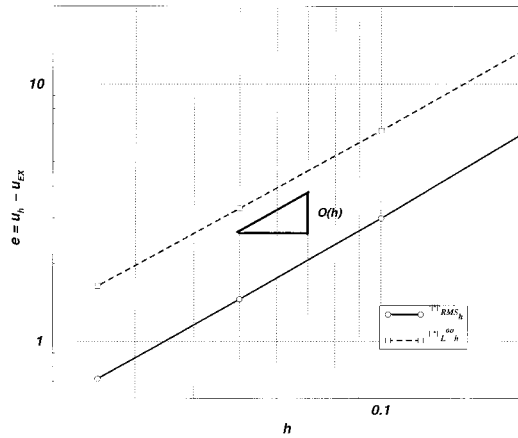FIG. 3.   Domain and boundary conditions for the Motz problem.

FIG. 4.   Motz problem—Error measures in $\Omega - \Omega_S$, $Ex = Ey = 0.4$.

in the sub-domain $\Omega - \Omega_S$, on a log–log scale. As expected, if no special treatment is applied to the FDS in the vicinity of the singular point, although the solution in $\Omega - \Omega_S$ is smooth, the convergence rate because of the ''pollution'' deteriorates considerably to $\mathcal{O}(h)$. It will be shown in the following that the Least-Square SFDS is ''pollution'' free.

SFDS with Collocation: We use the collocation technique only for this example problem to illustrate its behavior. Let us take a grid-mesh with $h = 0.2$ (i.e., $NGx = 11, NGy = 6$), $Ex = 2h$ and $Ey = 2h$ (see Fig. 5). Having a system of $50 + N$ equations, we compute the coefficients A_i of the asymptotic expansion (24) called GFIFs, when considering 1 then $2, 3, \cdots N$ coefficients in series. We summarize in Table I the first N coefficients A_i obtained by the collocation method, compared to the exact values from [22]. It is noticed that the convergence of GFIFs is not monotonic as N increases, and high accuracy for even large Ns (as $N = 6$, for example) is not guaranteed. Thus, unless one uses collocation for all points along Γ_S, the accuracy of the obtained values for the GFIFs cannot be guaranteed. There is also a strong dependency of the extracted GFIFs on the sub-domain size, which is a drawback of the collocation method in this example problem (the phenomenon has also been seen when considering a finer grid mesh). Numerical tests conducted also indicate that the accuracy of the extracted GFIFs is very sensitive to mesh size. For these reasons, the collocation method will be abandoned in favor of the Least-Squares SFDS, for which results are provided in the following.
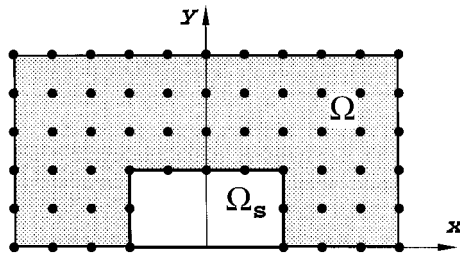

FIG. 5.   Grid for the Motz problem, $h = 0.2$, $Ex = 2h$, $Ey = 2h$.

TABLE I.   Values for A_i for the Motz problem, obtained by collocation, $h = 0.2, Ex = Ey = 2h$.

N	A_1	A_2	A_3	A_4	A_5	A_6	A_7
1	230.3618						
2	403.2672	76.9853					
3	403.1229	90.0322	21.4352				
4	400.9074	87.5280	17.0236	-8.1593			
5	399.5765	86.1002	14.4975	-11.0333	-3.5263		
6	397.3175	83.4513	10.9041	-16.7071	-8.1538	-5.6472	
7	401.1965	87.7603	17.4580	-7.9267	1.4419	1.9505	3.5630
Exact	401.1625	87.6559	17.2379	-8.0712	1.4403	0.3311	0.2754

Least-Squares SFDS: Results obtained by employing Least-Squares (L-S) SFDS are provided. Let us consider again a grid-mesh having $h = 0.2$ (i.e., $NGx = 11, NGy = 6$), with $Ex = 2h$ and $Ey = 2h$, as presented in Fig. 5. First, we demonstrate that when employing the L-S SFDS, the scheme is ''pollution'' free, i.e., it regains the $\mathcal{O}(h^6)$ convergence rate away from the singularity. Over the whole domain we use a grid-mesh containing NGx grid points in the x-direction and NGy points in the y-direction. Three different meshes are studied with $(NGx, NGy) = (11, 6), (21, 11), (41, 21)$. In the series, we use $N = 8, 13, 19$ terms, according to (22). Again, we plot the RMS_h measure of the error and the error in L_h^∞ norm in the sub-domain $\Omega - \Omega_S$, on a log–log scale in Fig. 6. Figure 6 clearly demonstrates that the Least-Squares SFDS is ''pollution'' free, i.e., the numerical scheme regained its $\mathcal{O}(h^6)$ convergence rate in $\Omega - \Omega_S$. More importantly, *the accuracy obtained with the Least-Squares SFDS has been improved by more than three orders of magnitude*, and the convergence rate over all Ω, *including the neighborhood of the singularity* is at least $\mathcal{O}(h^6)$.

Having three meshes with $(NGx, NGy) = (11, 6), (21, 11), (41, 21)$, and $Ex = 0.4$, we summarize in Table II the first six GFIFs, A_i when N is defined by (22). For example, for the mesh $(11, 6)$ one has to solve a system of $50 + 8$ equations and for the mesh $(21, 11)$, $185 + 13$
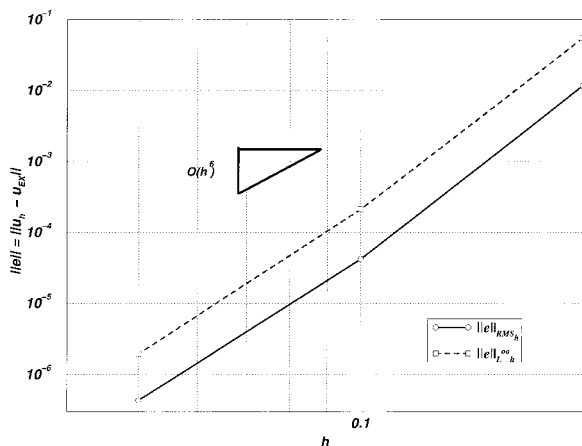

FIG. 6.   Motz problem with L-S SFDS: Error measures in $\Omega - \Omega_S, Ex = Ey = 0.4$.

TABLE II.   Values for A_i for the Motz problem, obtained by Least-Squares, $Ex = Ey = 0.4$.

Mesh	N	A_1	A_2	A_3	A_4	A_5	A_6
(11, 6)	8	401.1263375862	87.6612836028	17.2427839136	−8.4202285208	0.6598664045	0.3589950529
(21, 11)	13	401.1624857235	87.6558868625	17.2379085673	−8.0738056263	1.4401384896	0.3307413318
(41, 21)	19	401.1624541887	87.6559199742	17.2379153112	−8.0712413252	1.4402720290	0.3310543171
Exact		401.1624537452	87.6559201951	17.2379150794	−8.0712152597	1.4402727170	0.3310548859

equations. The absolute relative error (%) of the i-th GFIF is defined by

$$100\frac{|(A_{EX})_i - (A_h)_i|}{|(A_{EX})_i|}.$$

In Fig. 7, we plot the absolute relative error of the first six GFIFs on a log–log scale. One may notice that the convergence rate of the GFIFs is at least as fast as $\mathcal{O}(h^6)$, and very high accuracy (0.009% relative error) is obtained already at the coarsest mesh for A_1. As expected, the higher GFIFs are less accurate; however, from an engineering point of view only the first one or two GFIFs are of interest, and these are extremely accurate.

Next we investigate the influence of the size of the sub-domain Ω_S (characterized by the parameters Ex, Ey) on the accuracy of the extracted GFIFs. We consider three sizes of Ω_S all with $Ex = Ey$: $Ex = 0.4, Ex = 0.6$, and $Ex = 0.8$. As Ex increases, the number of grid points in $\Omega - \Omega_S$, for a given h, obviously decrease and at the same time the number of terms required in the series increases. For the mesh with $Ex = 0.6$ and $h = 0.2$, one has to solve a system of $42 + 13(= N)$ equations, and for $Ex = 0.6$ and $h = 0.1$, one has to solve a system of $149 + 22(= N)$ equations. For example, we summarize in Table III the extracted first GFIF for the various sizes of Ω_S for different hs. The absolute relative error (percentage) of the first three GFIFs as a function of Ex, for various hs (and corresponding Ns), is illustrated in Fig. 8. As Ω_S increases, the GFIFs are better approximated if the connection strategy in (22) is maintained. Extremely accurate GFIFs are obtained using minimal computational resources and a simplified L-S SFDS.

In [7] it is shown that the best approximations are obtained at $N = 35$, and that the stability of that method quickly deteriorates as N grows large. To verify the sensitivity of the present method in respect to the increase in N, we summarize in Table IV the relative errors in the first
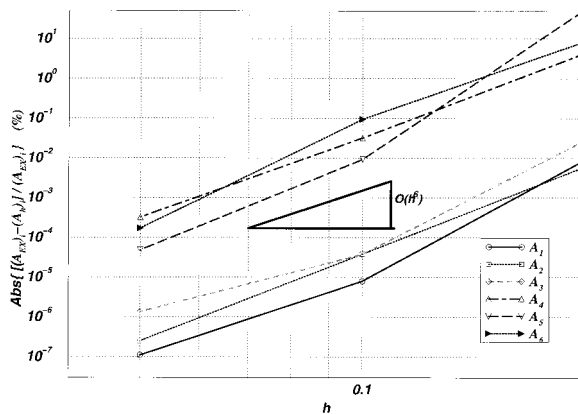

FIG. 7.   Motz problem with L-S SFDS: Convergence of the GFIFs, $Ex = Ey = 0.4$.

TABLE III.   Values for A_1 for the Motz problem, obtained by Least-Squares, for various $Ex = Ey$.

Ex h	0.2	0.1	0.05
0.4	401.126337586150	401.162485723470	401.162454188717
	$(N = 8)$	$(N = 13)$	$(N = 19)$
0.6	401.162613596063	401.162456095361	401.162453773681
	$(N = 12^a)$	$(N = 22)$	$(N = 32)$
0.8	401.162487292945	401.162454018793	401.162453748543
	$(N = 16^a)$	$(N = 32^a)$	$(N = 50)$

[a] According to (22) N had to be larger, but the number of grids along Γ_S was smaller than N.

five coefficients A_i as N increases up to 50, and the condition number of the matrix $[K]$, for $Ex = 0.8$. Table IV demonstrates that as N increases better results are obtained when coupled with a refinement in h, and that the condition number does not increase considerably even for $N = 50$.

B. Laplace Equation over an L-Shaped Domain

The domain is shown in Fig. 9. The boundary conditions are

$$u = 1 \text{ on } x = -1, -1 \leq y \leq 1$$

$$u = 0 \text{ on } x = 1, -1 \leq y \leq 0$$

$$\partial u/\partial n = 0 \text{ elsewhere on the boundary.}$$

$$(26)$$

The singularity arises from the re-entrant corner of magnitude $3\pi/2$ at the origin. The asymptotic expansion for the solution about the origin is of the form

$$u = \sum_{i=0}^{\infty} A_i r^{2i/3} \cos[(2i/3)\theta], \quad -3\pi/2 \leq \theta \leq 0. \tag{27}$$

Computations were carried out using a grid mesh of $h = 0.2$, with $Ex = Ey = 0.4 (N = 8)$, and the L-S SFDS. We are not aware of any exact values for the GFIFs, except another numerical calculation based on a singular-super-element and the h-version finite element method presented in [23], with which the current results could be compared. We list the GFIFs obtained by the L-S SFDS compared to those in [23] in Table V. We may conclude that the first four coefficients presented in Table V are accurate up to the shown 4 decimal digits.

C. Poisson Equation over an L-Shaped Domain

In this subsection the Poisson equation $\nabla^2 u = -1$, over the domain shown in Fig. 9 is considered, with homogeneous Dirichlet boundary conditions applied over the whole boundary. This problem concerns the fully developed Poiseuille flow in a duct of the L-shaped cross-section. The exact solution to this problem in the vicinity of the singular point consists of two parts: a homogeneous part u_H given by (27) (with sin instead of cos terms) and a particular solution [24]:

$$u_P(r,\theta) = r^2 \frac{-1}{3\pi} \left[\frac{3\pi}{4} - \ln(r)\cos(2\theta) + \theta\sin(2\theta) \right]. \tag{28}$$
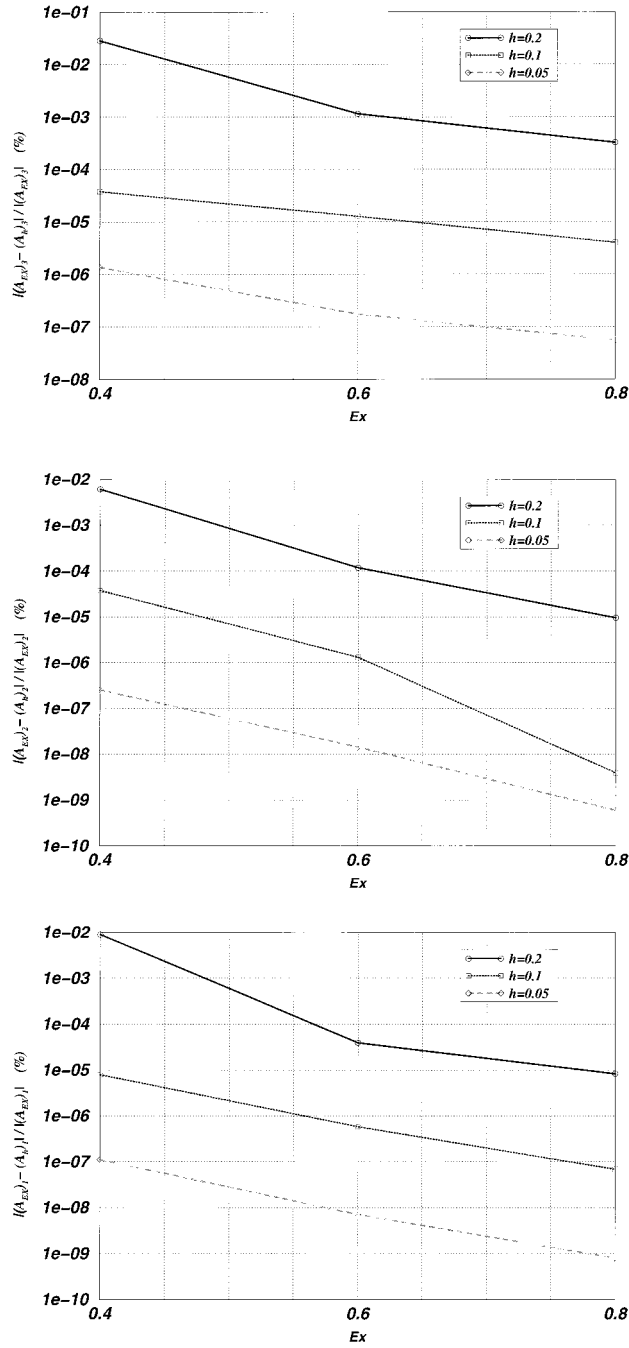
FIG. 8. Motz problem with L-S SFDS: Convergence of the GFIFs, for various ($Ex = Ey$).

$u = u_H + u_P$ also represents in engineering practice the Prantl's stress potential (see, e.g., [25, Chapter 35]) from which the stress tensor to the Saint Venant torsion of a straight bar can be

TABLE IV.   Relative errors in A_i for the Motz problem, obtained by Least-Squares at $Ex = Ey = 0.8$.

	$N = 16, h = 0.2$	$N = 32, h = 0.1$	$N = 50, h = 0.05$
$e_{A_1}(\%)$	$8.3626e - 06$	$6.8200e - 08$	$7.9873e - 10$
$e_{A_2}(\%)$	$9.5457e - 06$	$3.8992e - 09$	$8.6381e - 10$
$e_{A_3}(\%)$	$3.2480e - 04$	$3.9845e - 06$	$5.4001e - 08$
$e_{A_4}(\%)$	$4.6258e - 03$	$4.8031e - 05$	$5.9758e - 07$
$e_{A_5}(\%)$	$2.8341e - 03$	$4.1819e - 05$	$5.9397e - 07$
Cond. #[a]	$3.31e + 01$	$2.70e + 03$	$1.29e + 05$

[a] Cond. # $\stackrel{\text{def}}{=} \sqrt{\lambda_{\max}/\lambda_{\min}}$, where λ is an eigen-value of $[K]$.

obtained. This problem, for example, is of technical importance in fracture mechanics, and the ''stress intensity factor'' defined by $\frac{2}{3}A_1$ is often sought.

Exact solution to the problem of interest is not available; however, numerical tests using multi-grid methods are reported in [10]. According to this reference, $A_1 = 0.40192487$, which is accurate to the fourth significant digit, and $A_2 = \mathcal{O}(10^{-7})$. It is known [24] that, for the Poisson equation (with $f = 1$) over the L-shaped domain, the even terms in the expansion (27) vanish. Therefore we may expect that the computation will provide $A_2 = A_4 = \cdots = 0$.

We use three grid meshes with $h = 0.2, 0.1$, and 0.05 with $Ex = Ey = 0.4$, and N computed according to h and Ex. When applying the L-S SFDS for the Poisson equation, it is essential to consider the particular solution (28) as outlined in (19). For the mesh with $h = 0.2$, for example, one has to solve a system of $51 + 11(= N)$ equations. We summarize in Table VI the extracted first three GFIFs for the various meshes used together with the number of equations to be solved. We demonstrate that the first GFIFs are obtained accurately (up to the fifth digit) for the Poisson problem as well, and as expected $A_2 \approx 0$.
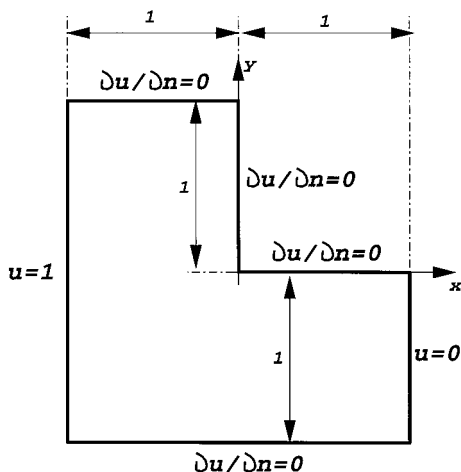

FIG. 9.   L-shaped domain and boundary conditions.

TABLE V.   Values for the GFIFs for the L-shaped domain.

	[23]	L-S SFDS
A_0	0.6667	0.6667
A_1	−0.4520	−0.4520
A_2	−0.2149	−0.2149
A_3	0.0000	0.0000

TABLE VI.   Values for A_1, A_2 and A_3 for the Poisson problem, obtained by L-S SFDS, for various grid meshes.

	$h = 0.2$ $51 + 11(= N)$ eqs.	$h = 0.1$ $228 + 20(= N)$ eqs.	$h = 0.05$ $960 + 28(= N)$ eqs.	[10]
A_1	0.401,928,540	0.401,937,293	0.401,931,091	0.40192487
A_2	$-3.6e - 17$	$1.1e - 16$	$-1.4e - 13$	$-1.475e - 7$
A_3	0.093,666,634	0.093,650,012	0.093,648,362	Not avail.

IV. SUMMARY AND CONCLUSIONS

Semi-analytic high-order finite difference schemes have been developed for two-dimensional elliptic boundary value problems with singularities in the solution arising from abrupt changes in the boundary conditions, or if the boundary has sharp corners. The emphasis in developing this scheme, called Least-Squares Singular Finite Difference Scheme (L-S SFDS), was devoted to a simple yet efficient and accurate scheme, which is two-fold: (a) the scheme is ''pollution'' free, i.e., no degradation in convergence rate is visible because of the singularities; and (b) the generalized flux intensity factors are computed as a by-product with a very high accuracy.

Application to test problems for the Laplace and Poisson equations show the L-S SFDS to be both accurate and efficient. The computation yields values for the coefficients in the asymptotic series representing the solution in the vicinity of the singular point, as well as for the solution over the rest of the domain. The generalized flux intensity factors, which are the coefficients of the asymptotic expansion and are of particular practical importance in many engineering applications, are obtained with very high accuracy.

The method may be extended to elliptic problems involving other types of singularities, such as those caused by an interface between two different elastic materials, for example, provided that the form of the asymptotic series for the solution in the vicinity of the singular point is known.

References

1. L. Collatz, *The Numerical Treatment of Differential Equations,* Springer–Verlag, Berlin, 1960.

2. D. M. Young and R. T. Gregory, *A Survey of Numerical Mathematics—Vol. 2,* Addison–Wesley, 1973.

3. R. E. Lynch and J. R. Rice, ''The Hodie method and its performance for solving elliptic partial differential equations,'' in *Recent Developments in Numerical Analysis,* C. de Boor, Ed., Academic Press, New York, pp. 143–175, 1978.

4. R. F. Boisvert, ''Families of high order accurate discretizations of some elliptic problems,'' *SIAM J. Sci. Stat. Comput.* **2,** 268–284 (1981).

5. M. M. Gupta, R. Manohar, and J. W. Stephenson, ''High-order difference scheme for two-dimensional elliptic equations,'' *Numer. Meth. Partial Differential Eq.* **1,** 71–80 (1985).

6. C. Zenger and H. Gietl, ''Improved difference schemes for the Dirichlet problem of the Poisson equation in the neighborhood of corners,'' *Numerische Mathematik* **30,** 315–332 (1978).

7. Z-C. Li, R. Mathon, and P. Sermer, ''Boundary methods for solving elliptic problems with singularities and interfaces,'' *SIAM J. Num. Anal.* **24,** 487–498 (1987).

8. X. Wu and H. Han, ''A finite element method for Laplace and Helmholtz-type boundary value problems with singularities,'' *SIAM Jour. Numer. Anal.* **34,** 1037–1050 (1997).

9. H. Motz, ''The treatment of singularities of partial differential equations by relaxation methods,'' *Quart. Appl. Math.* **4,** 371 (1946).

10. C. Susanne Brenner, ''Multigrid methods for the computation of singular solutions and stress intensity factors I: Corner singularities,'' *Math. Comp.* 1996, preprint.

11. V. A. Kondratiev, ''Boundary value problems for elliptic equations in domains with conical or angular points,'' *Transact. Moscow Math. Soc.* **16,** 227–313 (1967).

12. P. Grisvard, *Elliptic Problems in Nonsmooth Domains,* Pitman, England, 1985.

13. D. Leguillon and E. Sanchez–Palencia, *Computation of Singular Solutions in Elliptic Problems and Elasticity,* John Wiley & Sons, New York, 1987.

14. P. Papadakis and I. Babuška, ''A numerical procedure for the determination of certain quantities related to stress intensity factors in two-dimensional elasticity,'' *Computer Meth. Appl. Mech. Engrg.* **122,** 69–92 (1995).

15. M. Costabel and M. Dauge, ''Computation of corner singularities in linear elasticity,'' in *Boundary value problems and integral equations in nonsmooth domains,* M. Costabel, M. Dauge, and S. Nicaise, Eds., Marcel Dekker, New York, Basel, Hong-Kong, pp. 59–68, 1995.

16. Z. Yosibash and B. A. Szabó, ''Numerical analysis of singularities in two-dimensions. Part 1: Computation of eigenpairs,'' *Int. J. Numer. Meth. Engrg.* **38,** 2055–2082 (1995).

17. D. Gilbarg and N. S. Trudinger, *Elliptic Partial Differential Equations of Second Order,* Springer–Verlag, Berlin, Heidelberg, New York, 1977.

18. G. Strang and G. J. Fix, *An analysis of the finite element method,* Prentice–Hall, Englewood, NJ, 1973.

19. L. V. Kantorovich and V. I. Krylov, *Approximation Methods of Higher Analysis,* Interscience, New York, 1964.

20. M. Arad, A. Yakhot, and G. Ben-Dor, ''A highly accurate numerical solution of a biharmonic equation,'' *Num. Meth. Partial Differential Eqs.,* to appear.

21. P. Laasonen, ''On the discretization error of the Dirichlet problem in a plane region with corners,'' *Ann. Acad. Sci. Fenn. Ser. A,* **408,** 1–16 (1967).

22. J. B. Rosser and N. Papamichael, ''A power series solution of a harmonic mixed boundary value problem,'' *MRC Technical Summary,* Rept. 1405, Univ. of Wisconsin, 1975.

23. Z. Yosibash and B. Schiff, ''Super-elements for the finite element solution of two-dimensional elliptic problems with boundary singularities,'' *Finite Elements in Analysis and Design* **26,** 315–335 (1997).

24. H. K. Moffatt and B. R. Duffy, ''Local similarity solutions and their limitations,'' *J. Fluid Mech.* **96,** 299–313 (1980).

25. I. S. Sokolnikoff, *Mathematical Theory of Elasticity,* McGraw–Hill, New York, 1956.